Ain Shams Engineering Journal (2016) 7, 593–602

Ain Shams University

Ain Shams Engineering Journal

www.elsevier.com/locate/asej
www.sciencedirect.com

ENGINEERING PHYSICS AND MATHEMATICS

Magnetohydrodynamic flow of a Casson fluid over an exponentially inclined permeable stretching surface with thermal radiation and chemical reaction

P. Bala Anki Reddy *

Fluid Dynamics Division, School of Advanced Sciences, VIT University, Vellore, T.N. 632014, India

Received 2 November 2014; revised 19 November 2015; accepted 9 December 2015
Available online 16 February 2016

KEYWORDS

Casson fluid;
MHD;
Porous medium;
Inclined stretching sheet;
Thermal radiation;
Chemical reaction and suction/blowing

Abstract This article investigates the theoretical study of the steady two-dimensional MHD convective boundary layer flow of a Casson fluid over an exponentially inclined permeable stretching surface in the presence of thermal radiation and chemical reaction. The stretching velocity, wall temperature and wall concentration are assumed to vary according to specific exponential form. Velocity slip, thermal slip, solutal slip, thermal radiation, chemical reaction and suction/blowing are taken into account. The proposed model considers both assisting and opposing buoyant flows. The non-linear partial differential equations of the governing flow are converted into a system of coupled non-linear ordinary differential equations by using the similarity transformations, which are then solved numerically by shooting method with fourth order Runge–Kutta scheme. The numerical solutions for pertinent parameters on the dimensionless velocity, temperature, concentration, skin friction coefficient, the heat transfer coefficient and the Sherwood number are illustrated in tabular form and are discussed graphically.

1. Introduction

The theory of non-Newtonian fluid flow over a stretching surface has become a field of active research for the last few decades due to its wide range of applications in technology and industry. Such applications include polymer extrusion from a dye, wire drawing, the boundary layer along a liquid film in condensation processes, glass blowing, paper production, artificial fibers, hot rolling, cooling of metallic sheets or electronic chips, food stuffs, slurries and many others. Many researchers and scientists [1–9] analyzed the boundary layer flow over a stretching surface on various non-Newtonian models. The various non-Newtonian fluids are power-law fluids, micropolar fluids, viscoelastic fluids, Jeffrey fluid, Rivlin-Ericksen fluids, Casson fluids, Walter's liquid B fluids etc. Although various types of non-Newtonian fluid models are

* Tel.: +91 8500132515.
E-mail addresses: pbarmaths@gmail.com, pbarsvu@gmail.com
Peer review under responsibility of Ain Shams University.

Production and hosting by Elsevier

http://dx.doi.org/10.1016/j.asej.2015.12.010

Nomenclature

U	stretching velocity
U_0	reference velocity
T_0	reference temperature
C_0	reference concentration
L	reference length
B_0	constant
P_y	yield stress of the fluid
u	velocity component in the x direction (ms^{-1})
v	velocity component in the y direction (ms^{-1})
x, y	coordinates along and normal to the stretching surface (m)
p	fluid pressure
g	acceleration due to gravity
c_p	specific heat at constant pressure ($J\,kg^{-1}\,k^{-1}$)
k	thermal conductivity ($w\,m^{-1}\,k^{-1}$)
k'	dimensional permeability
T	temperature of the fluid (K)
T_w	surface temperature
C_w	surface concentration
T_∞	temperature far away from the stretching sheet
C	concentration of the fluid ($kmol\,m^{-3}$)
C_∞	concentration of the ambient fluid
q_r	radiative heat flux
D	mass diffusion coefficient ($m^2\,s^{-1}$)
k^*	Rosseland mean absorption coefficient
H	magnetic parameter
K	permeability parameter
Gr	local Grashof number
Gc	local solutal Grashof number
R	radiation parameter
Pr	Prandtl number
Sc	Schmidt number
S	suction parameter
N	velocity slip factor
M	thermal slip factor
P	solutal slip factor
V	velocity at the wall
N_1	constant
M_1	constant
P_1	constant
S_v	non dimensional velocity slip
S_t	non dimensional thermal slip
S_c	non dimensional solutal slip
q_w	surface heat flux
J_w	mass flux
C_f	skin friction coefficient
Nu_x	local Nusselt number
Sh_x	local Sherwood number
Re_x	local Reynolds number

Greek symbols

μ_B	plastic dynamic viscosity of the non-Newtonian fluid
π $(i,j)th$	component of the deformation rate
π_c	critical value of this product based on the non-Newtonian model
υ	kinematic viscosity
ρ	density of the fluid ($kg\,m^{-3}$)
β	Casson parameter
σ	electrical conductivity
β_T	coefficient of thermal expansion (m^3/kmol)
β^*	coefficient of solutal expansion (K^{-1})
α	inclination angle from the vertical direction
σ^*	Stefan–Boltzmann constant
λ	buoyancy parameter
η	similarity variable
δ	solutal buoyancy parameter
θ	dimensionless temperature
ϕ	dimensionless concentration
Γ	chemical reaction rate ($kmol\,m^{-3}$)
γ	chemical reaction parameter
τ_w	surface shear stress ($N\,m^{-2}$)

Subscripts

w	conditions at the wall
∞	ambient condition

Superscript

$'$	differentiation with respect to η

proposed to explain the behavior, one of the most important types of non-Newtonian fluids is the Casson fluid. The Casson fluid is a plastic fluid, which yields shear stress in Constitutive equations. Some of the examples of Casson fluid model are jelly, soup, honey, tomato sauce, concentrated fruit juices, drilling operations, food processing, metallurgy, paints, coal in water, synthetic lubricants, manufacturing of pharmaceutical products, synovial fluids, sewage sludge and many others. Human blood is also considered as Casson fluid because of the presence of several substances like protein, fibrinogen and globin in aqueous base plasma in the blood. Human red cells from a chain like structure, known as aggregates or rouleaux. If the rouleaux behave like a plastic solid then there exists a field stress that can be identified with the constant stress in Casson fluid [10]. Majority of researchers [11–20] analyzed the Casson fluid flow over a stretching sheet. Recently, the steady stagnation point flow Casson nano fluid over a convective stretching surface is examined by Nadeem et al. [21].

Thermal radiation and chemical reaction effects on heat and mass transfer over a stretching surface play an important role in Physics and Engineering due to its wide range applications, such as Nuclear power plants, combustion of fossil fuels, liquid metal fluids, gas turbines, plasma wind tunnels, photo ionization, geophysics, and the various propulsion devices for missiles, aircraft, space vehicles, and satellites. The effects of thermal radiation over a stretching sheet under different flow conditions have been reported by several researchers [22–34]. Very recently, the numerical solutions for steady boundary layer flow and heat transfer for a Casson fluid over an exponentially permeable stretching surface in the presence of thermal radiation are analyzed by Pramanik [35].

To the best of author knowledge, no investigation has been made yet to analyze the magnetohydrodynamic convective boundary layer flow of a Casson fluid over an exponentially inclined permeable stretching surface in the presence of thermal radiation and chemical reaction. The present work aims to fill the gap in the existing literature. Motivated by the above studies, a mathematical model is presented here to understand the effects of slips, thermal radiation and chemical reaction on MHD boundary layer flow of Casson fluid over an inclined exponentially stretching surface. The coupled partial differential equations of the governing flow are transformed into nonlinear coupled ordinary differential equations by a similarity transformation. The resulting nonlinear coupled differential equations are solved numerically by using fourth order Runge–Kutta scheme together with shooting method. This paper has been arranged as follows: Section 2 deals with the mathematical formulation of the problem. The method of solution is given in Section 3. Section 4 comprises of results and discussions. The concluding remarks are presented in Section 5.

2. Mathematical analysis

Consider two dimensional flow of an incompressible viscous electrically conducting Casson fluid over an exponentially permeable stretching sheet which is inclined with an acute angle α to the vertical. The x-axis is taken along the stretching surface in the direction of the motion while the y-axis is perpendicular to the surface which is shown in Fig. 1. The stretching surface has the velocity $U = U_0 e^{\frac{x}{L}}$, the temperature distribution $T_w = T_\infty + T_0 e^{\frac{x}{L}}$ and the concentration distribution $C_w = C_\infty + C_0 e^{\frac{x}{L}}$ where U_0 is the reference velocity, T_0 is the reference temperature, C_0 is the reference concentration and L is the reference length. A variable magnetic field $B = B_0 e^{\frac{x}{2L}}$ is applied normal to the sheet, where B_0 is a constant.

We assume that the rheological equation of state for an isotropic and incompressible flow of a Casson fluid is as [18,35]:

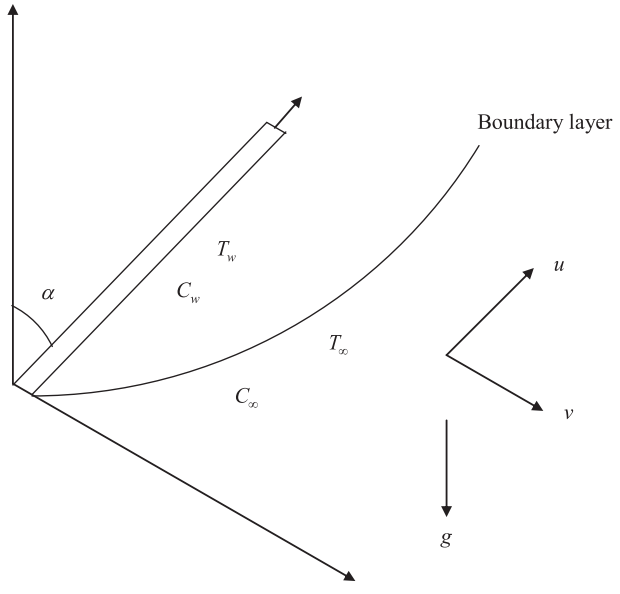

Figure 1 Sketch of the physical flow problem.

$$\tau_{ij} = \begin{cases} 2(\mu_B + P_y/\sqrt{2\pi})e_{ij}, \pi > \pi_c \\ 2(\mu_B + P_y/\sqrt{2\pi_c})e_{ij}, \pi < \pi_c \end{cases}$$

where μ_B is the plastic dynamic viscosity of the non-Newtonian fluid, P_y is the yield stress of the fluid, $\pi = e_{ij}e_{ij}$, e_{ij} is the $(i,j)th$ component of the deformation rate and π_c is the critical value of this product based on the non-Newtonian model.

The continuity, momentum, energy and concentration equations governing such type of flow can be written as

$$\frac{\partial u}{\partial x} + \frac{\partial v}{\partial y} = 0, \tag{1}$$

$$u\frac{\partial u}{\partial x} + v\frac{\partial u}{\partial y} = -\frac{1}{\rho}\frac{\partial p}{\partial x} + \upsilon\left(1+\frac{1}{\beta}\right)\left(\frac{\partial^2 u}{\partial x^2} + \frac{\partial^2 u}{\partial y^2}\right) - \frac{\sigma B^2}{\rho}u - \frac{\upsilon}{k'}u \pm g\beta_T(T - T_\infty)\cos\alpha + g\beta^*(C - C_\infty)\cos\alpha, \tag{2}$$

$$u\frac{\partial v}{\partial x} + v\frac{\partial v}{\partial y} = -\frac{1}{\rho}\frac{\partial p}{\partial y} + \upsilon\left(1+\frac{1}{\beta}\right)\left(\frac{\partial^2 u}{\partial x^2} + \frac{\partial^2 u}{\partial y^2}\right), \tag{3}$$

$$u\frac{\partial T}{\partial x} + v\frac{\partial T}{\partial y} = \frac{k}{\rho c_p}\frac{\partial^2 T}{\partial y^2} - \frac{1}{\rho c_p}\frac{\partial q_r}{\partial y}, \tag{4}$$

$$u\frac{\partial C}{\partial x} + v\frac{\partial C}{\partial y} = D\frac{\partial^2 C}{\partial y^2} - \Gamma(C - C_\infty). \tag{5}$$

Subject to the boundary conditions:

$$u = U + N\mu\frac{\partial u}{\partial y}, v = -V(x), T = T_w + M\frac{\partial T}{\partial y}, C = C_w + P\frac{\partial C}{\partial y} \quad \text{at } y = 0$$
$$u \to 0, T \to T_\infty, C \to C_\infty \quad \text{as } y \to \infty. \tag{6}$$

Here $N = N_1 e^{\frac{-x}{L}}$ is the velocity slip factor, $M = M_1 e^{\frac{-x}{L}}$ is the thermal slip factor and $P = P_1 e^{\frac{-x}{L}}$ is the solutal slip factor. The no-slip conditions can be recovered, by considering $N = M = P = 0$. It is assumed that the permeability is in the form of $k' = k_1 e^{\frac{-x}{L}}$ and the reaction rate is in the form of $\Gamma = k_0 e^{\frac{x}{L}}$. Where u and v are the velocity components in the x and y directions respectively, υ is the kinematic viscosity, ρ is the density of the fluid, β is the Casson parameter, σ is the electrical conductivity, g is the acceleration due to gravity, β_T is the coefficient of thermal expansion, β^* coefficient of solutal expansion, T is the temperature, T_∞ is the temperature of the ambient fluid, C is the concentration, C_∞ is the concentration of the ambient fluid, c_p is the specific heat at constant pressure, k is the thermal conductivity, q_r is the radiative heat flux and D is the mass diffusion coefficient. Also, + sign and − sign in Eq. (2) correspond to assisting buoyant flow and opposing buoyant flow respectively.

Thermal radiation is simulated using the Rosseland diffusion approximation and in accordance with this, the radiative heat flux q_r is given by

$$q_r = -\frac{4\sigma^*}{3k^*}\frac{\partial T^4}{\partial y}. \tag{7}$$

where σ^* is the Stefan–Boltzmann constant and k^* is the Rosseland mean absorption coefficient. If the temperature differences within the mass are sufficiently small, then Eq. (7) can be linearized by expanding T^4 into the Taylor's series about T_∞ and neglecting higher order terms, we get

$$T^4 \cong 4T_\infty^3 T - 3T_\infty^4. \tag{8}$$

Using Eqs. (7) and (8), Eq. (4) can be written as

$$u\frac{\partial T}{\partial x} + v\frac{\partial T}{\partial y} = \left(\frac{k}{\rho c_p} + \frac{16\sigma^* T_\infty^3}{3\rho C_p k^*}\right)\frac{\partial^2 T}{\partial y^2}. \tag{9}$$

We introduce the similarity variables as

$$\begin{aligned} &\eta = \left(\frac{U_0}{2\upsilon L}\right)^{\frac{1}{2}} e^{\frac{x}{2L}} y, u = U_0 e^{\frac{x}{L}} f'(\eta), \\ &v = -\sqrt{\frac{\upsilon U_0}{2L}} e^{\frac{x}{2L}}(f(\eta) + \eta f'(\eta)), T = T_\infty + T_0 e^{\frac{x}{2L}}\theta(\eta), \\ &C = C_\infty + C_0 e^{\frac{x}{2L}}\phi(\eta). \end{aligned} \tag{10}$$

The pressure outside the boundary layer in quiescent part of flow is constant and the flow occurs only due to the stretching of the sheet and hence the pressure gradient can be neglected. Considering the usual boundary layer approximations, $u \gg v, \frac{\partial u}{\partial y} \gg \frac{\partial u}{\partial x}, \frac{\partial v}{\partial y}, \frac{\partial v}{\partial y}$, the momentum equation in y-direction reduces to $\frac{\partial p}{\partial y} = 0$. Now substituting (10) into the Eqs. (2, 5 and 9), we get the following set of ordinary differential equations

$$\left(1 + \frac{1}{\beta}\right) f''' + ff'' - 2(f')^2 - (H + K)f' \pm \lambda\theta\cos\alpha + \delta\phi\cos\alpha = 0, \tag{11}$$

$$\left(1 + \frac{4}{3}R\right)\theta'' + Pr(f\theta' - f'\theta) = 0, \tag{12}$$

$$\phi'' + Sc(f\phi' - f'\phi) - Sc\gamma\phi = 0. \tag{13}$$

with the boundary conditions

$$\begin{aligned} &f = S, f' = 1 + S_v f''(0), \theta = 1 + S_t\theta'(0), \phi = 1 + S_c\phi'(0) \quad \text{at } \eta = 0 \\ &f' \to 0, \theta \to 0, \phi \to 0 \quad \text{as } \eta \to \infty. \end{aligned} \tag{14}$$

where the prime denotes differentiation with respect to η, $H = \frac{2\sigma B_0^2 L}{\rho U_0}$ is the magnetic parameter, $K = \frac{2\upsilon L}{k_1 U_0}$ is the permeability parameter, $Gr = \frac{2g\beta_T(T_w - T_\infty)Lx^2}{\upsilon^2}$ is the local Grashof number, $\lambda = \frac{Gr}{Re_x^2}$ is the buoyancy parameter, $Gc = \frac{2g\beta^*(C_w - C_\infty)Lx^2}{\upsilon^2}$ is the local solutal Grashof number, $\delta = \frac{Gc}{Re_x^2}$ is the solutal buoyancy parameter, $R = \frac{4\sigma^* T_\infty^3}{kk^*}$ is the radiation parameter, $Pr = \frac{\mu c_p}{k}$ is the Prandtl number, $Sc = \frac{\upsilon}{D}$ is the Schmidt number, $\gamma = \frac{2Lk_0}{U_0}$ is the chemical reaction parameter, $S = \frac{V_0}{\sqrt{\frac{U_0\upsilon}{2L}}} > 0$ (or < 0) is the suction (or blowing).The non-dimensional velocity slip S_v, thermal slip S_t and solutal slip S_c are defined by

$$S_v = N_1\rho\sqrt{\frac{\upsilon U_0}{2L}}, S_t = M_1\sqrt{\frac{U_0}{2\upsilon L}} \text{ and } S_c = P_1\sqrt{\frac{U_0}{2\upsilon L}}. \tag{15}$$

The quantities of physical interest in this problem are the skin-friction coefficient, heat transfer rate and mass transfer, which are defined as

$$C_f = \frac{2\tau_w}{\rho U_0^2 e^{\frac{2x}{L}}}, Nu_x = \frac{xq_w}{k(T_w - T_\infty)} \text{ and } Sh_x = \frac{xJ_w}{D(C_w - C_\infty)}. \tag{16}$$

The surface shear stress τ_w, surface heat flux q_w and mass flux J_w are given by

$$\tau_w = \mu\left(\frac{\partial u}{\partial y}\right)_{y=0}, q_w = -k\left(\frac{\partial T}{\partial y}\right)_{y=0} \text{ and } J_w = -D\left(\frac{\partial C}{\partial y}\right)_{y=0}. \tag{17}$$

Substituting (10) and (17) into Eq. (16), we get

$$\frac{C_f\sqrt{Re_x/2}}{\sqrt{x/L}} = f''(0), \frac{Nu_x}{\sqrt{Re_x/2}\sqrt{x/L}} = -\theta'(0) \text{ and } \frac{Sh_x}{\sqrt{Re_x/2}\sqrt{x/L}} = -\phi'(0). \tag{18}$$

where $Re_x = \frac{xU_0 e^{\frac{x}{L}}}{\upsilon}$ is the local Reynolds number. The above Skin-friction coefficient, local Nusselt number and Sherwood number shows that its variation depends on the variation of the factors $f''(0), -\theta'(0)$ and $-\phi'(0)$ respectively.

3. Method of solution

Eqs. (11–13) along with the boundary conditions (14) form a two point boundary value problem. These equations are solved using shooting method, by converting them to an initial value problem. For this, we transform the non-linear ordinary differential Eqs. (11–13) to a system of first order differential equations as follows:

$$\begin{aligned} &f' = z, z' = p, \\ &p' = \left(\frac{\beta}{1+\beta}\right)(2z^2 - fp + (H + K)z \mp \lambda\theta\cos\alpha - \delta\phi\cos\alpha), \end{aligned} \tag{19}$$

$$\begin{aligned} &\theta' = q, \\ &q' = -\left(\frac{3Pr}{4R + 3}\right)(fq - z\theta), \end{aligned} \tag{20}$$

$$\begin{aligned} &\phi' = r, \\ &r' = -sc(fr - bz\phi - \gamma\phi). \end{aligned} \tag{21}$$

The boundary conditions (14) become

$$\begin{aligned} f(0) = s, f'(0) &= 1 + s_v\omega_1, \omega_1 = f''(0), \theta(0) \\ &= 1 + s_t\omega_2, \omega_2 = \theta'(0), \phi(0) = 1 + s_c\omega_3, \omega_3 = \phi'(0). \end{aligned} \tag{22}$$

In order to integrate (19)–(21) as an initial value problem, we require values of $p(0)$ i.e., $f''(0)$, $q(0)$ i.e., $\theta'(0)$ and $r(0)$ i.e., $\phi'(0)$. But no such values are given at the boundary. So the suitable guess values for $f''(0), \theta'(0)$ and $\phi'(0)$ are chosen and then integration is carried out. The most important factor of the shooting method is to choose an appropriate finite value of η_∞. In order to determine η_∞ for the boundary value problem, start with some initial guess values for some particular set of physical parameters to obtain $f''(0), \theta'(0)$ and $\phi'(0)$. The solving procedure is repeated with another large value of η_∞ until two successive values of $f''(0), \theta'(0)$ and $\phi'(0)$ differ only by the specified significant digit. The last value of η_∞ is finally chosen to be the most appropriate value of the limit η_∞ for that particular set of parameters. The value of η_∞ may change for another set of physical parameters. Once the finite value of

η_∞ is determined, then the integration is carried out. Compare the calculated values for f', θ and ϕ at $\eta = 10$ (say) with the given boundary conditions $f'(10) = 0, \theta(10) = 0,\ \phi(10) = 0$ and adjust the estimated values, $f''(0), \theta'(0)$ and $\phi'(0)$ to give better approximation to the solution. We take the series values for $f''(0), \theta'(0), \phi'(0)$ and apply the fourth order Runge–Kutta method with step size $h = 0.01$ [35]. The above procedure is repeated until to get the results up to the desired degree of accuracy 10^{-6}.

4. Results and discussion

To assess the validity and accuracy of the applied numerical scheme, numerical values for the heat transfer coefficient for various values of thermal radiation and the Prandtl number in the absence of Casson fluid parameter, magnetic parameter, permeability parameter, buoyancy parameter, solutal buoyancy parameter, inclination parameter, thermal radiation, Schmidt number, suction parameter, velocity slip, thermal slip and solutal slip are compared with the available results and the outcome is shown in Table 1. The results are found in excellent agreement. In this study, the default values of the various parameters which we considered are:

$$\beta = 2.0, M = 1.0, K = 1.0, \lambda = 6.0, \delta = 6.0, \alpha = \frac{\pi}{4}, R = 0.5,$$

$$Pr = 0.72, Sc = 0.60, \gamma = 0.5, S_v = S_t = S_c = 0.1 \text{ and } S = 0.5.$$

Table 3 The values of skin friction coefficient, Nusselt number and the Sherwood number for various values of R, Pr, S_t, Sc, γ and S_c.

R	Pr	S_t	Sc	γ	S_c	$f''(0)$	$-\theta'(0)$	$-\phi'(0)$
0.5	0.7	0.1	0.6	0.5	0.1	0.15736	0.79962	1.10057
1.0	0.7	0.1	0.6	0.5	0.1	0.22232	0.66738	1.11153
0.5	1.0	0.1	0.6	0.5	0.1	0.08692	0.95717	1.08892
0.5	0.7	0.3	0.6	0.5	0.1	0.05709	0.68413	1.09131
0.5	0.7	0.1	1.0	0.5	0.1	0.04968	0.78189	1.43450
0.5	0.7	0.1	0.6	1.0	0.1	0.12438	0.79411	1.20277
0.5	0.7	0.1	0.6	0.5	0.3	0.04595	0.78983	0.89597

The effects of the pertinent parameters, namely, magnetic parameter, permeability parameter, Casson parameter, buoyancy parameter, solutal buoyancy parameter, inclination parameter, radiation parameter, Prandtl number, Schmidt number, chemical reaction parameter, velocity slip, thermal slip, solutal slip and suction parameter on the dimensionless velocity, temperature and concentration for three cases (i) assisting, (ii) opposing and (iii) blowing are shown in Figs. 2–16. The influences of the skin friction coefficient, Nusselt number and the Sherwood number are presented in Tables 2 and 3.

The influences of magnetic parameter on the velocity profiles are depicted in Fig. 2. It is observed that the velocity

Table 1 Comparison $-\theta'(0)$ for several values of Prandtl number and thermal radiation in the absence of Casson fluid parameter, magnetic parameter, permeability parameter, buoyancy parameter, solutal buoyancy parameter, Schmidt number, suction parameter, velocity slip, thermal slip and solutal slip.

Pr	R	Nadeem et al. [4]	Bidin and Nazar [22]	Magyari and Keller [23]	Mukhopadhyay and Reddy [24]	Ishak [25]	Pramanik [35]	Present
1	0		0.9547	0.954782	0.9547	0.9548	0.9547	0.95477
2	0		1.4714		1.4714	1.4715	1.4714	1.47144
3	0		1.8691	1.869075	1.8691	1.8691	1.8691	1.86916
5	0		1.1599	2.500135	2.5001	2.5001	2.5001	2.50016
10	0			3.660379	3.6603	3.6604	3.6603	3.66038
1	0.5	0.680	0.6765		0.6765		0.6765	0.67650
1	1.0	0.534	0.5315		0.5315		0.5315	0.53150
2	0.5	1.073	1.0735		1.0734		1.0734	1.07350
2	1.0	0.863	0.8627		0.8626		0.8626	0.86270
3	0.5	1.381	1.3807		1.3807		1.3807	1.38070
3	1.0	1.121	1.1214		1.1213		1.1213	1.12140

Table 2 The values of skin friction coefficient, Nusselt number and the Sherwood number for various values of β, H, K, λ, δ, α, S and S_v.

β	H	K	λ	δ	α	S	S_v	$f''(0)$	$-\theta'(0)$	$-\phi'(0)$
2.0	1.0	1.0	6.0	6.0	$\pi/4$	0.5	0.1	0.15736	0.79962	1.10057
3.0	1.0	1.0	6.0	6.0	$\pi/4$	0.5	0.1	0.19991	0.80047	1.10200
2.0	1.5	1.0	6.0	6.0	$\pi/4$	0.5	0.1	0.04237	0.78575	1.08881
2.0	1.0	1.5	6.0	6.0	$\pi/4$	1.0	0.1	0.04237	0.78575	1.08881
2.0	1.0	1.0	7.0	6.0	$\pi/4$	0.5	0.1	0.27756	0.81189	1.11132
2.0	1.0	1.0	6.0	7.0	$\pi/4$	0.5	0.1	0.25941	0.80836	1.10862
2.0	1.0	1.0	6.0	6.0	$\pi/2$	0.5	0.1	−1.43935	0.56834	0.91460
2.0	1.0	1.0	6.0	6.0	$\pi/4$	1.0	0.1	0.00244	0.89797	1.23430
2.0	1.0	1.0	6.0	6.0	$\pi/4$	0.5	0.3	0.11324	0.80222	1.10351

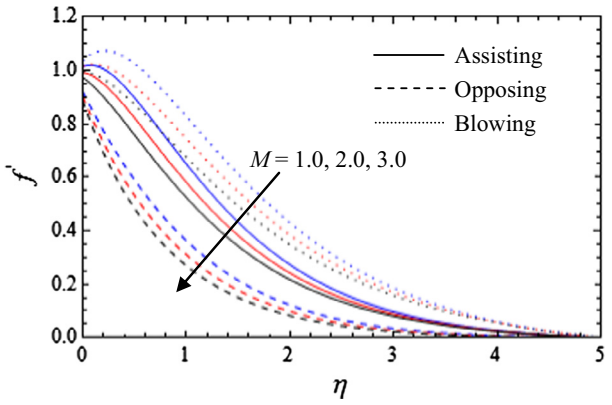

Figure 2 Velocity profiles for various values of M.

decreases as magnetic parameter increases for the cases of assisting, opposing and blowing. This is due to the fact that an increase in M signifies an enhancement of Lorentz force, thereby reducing the magnitude of the velocity [26]. The variation of dimensionless velocity distribution for different values of permeability parameter is shown in Fig. 3. It is observed that the velocity of the fluid decreases with increase in the permeability parameter. Fig. 4 displays the effect of inclination parameter on the velocity profiles. From Fig. 4 we infer that, the velocity profiles decrease with an increase in the inclination parameter. This can be attributed to the fact that the angle of inclination decreases the effect of the buoyancy force due to thermal diffusion by a factor of $\cos\alpha$. Consequently, the driving force to the fluid decreases as a result velocity of the fluid decreases [32]. The effects of the Casson fluid parameter on the velocity for the cases of assisting, opposing and blowing are presented in Fig. 5. It is observed that in the case of assisting and opposing flows, the velocity increases at the beginning but it decreases after a certain distance η normal to the sheet. It is further noticed that the velocity decreases for the case of blowing. Some characteristic velocity profiles for different values of solutal buoyancy parameter are presented in Fig. 6. It can be seen that the velocity increases with an increase in solutal buoyancy parameter for the three cases. Effects of velocity slip on the velocity profiles are shown in Fig. 7. It is observed that the velocity increases for the cases of assisting and blowing, whereas the reverse trend is found in the case of opposing flow.

The effect of magnetic parameter on the temperature profiles is depicted in Fig. 8, which describes an increase in the magnetic parameter enhances the temperature profiles. This enhancement can be attributed to the fact that the introduction of the transverse magnetic field to an electrically conducting fluid gives rise to a resistive type of force known as Lorentz force. This force bears the potential to enhance the temperature of the fluid [26]. The temperature field is shown

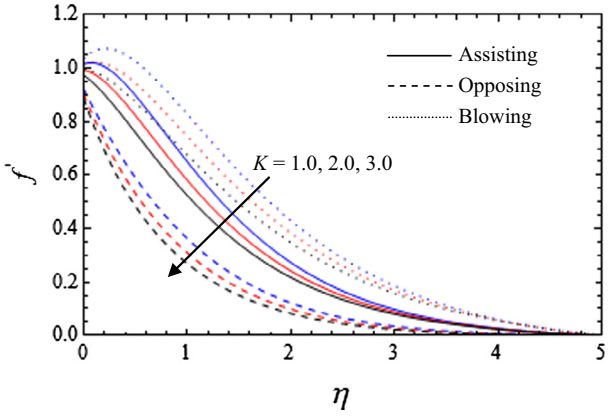

Figure 3 Velocity profiles for various values of k.

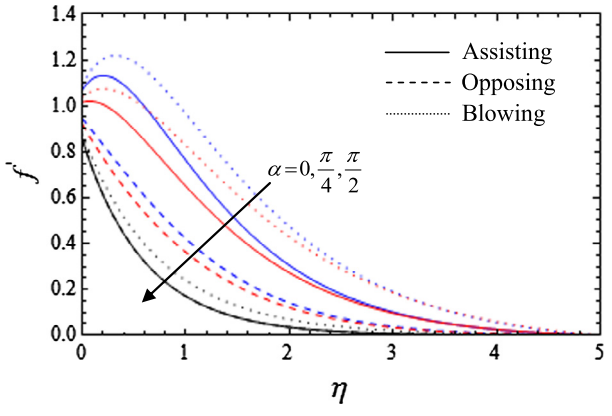

Figure 4 Velocity profiles for various values of α.

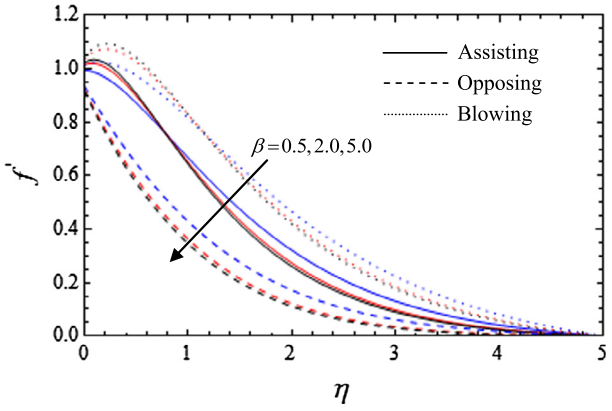

Figure 5 Velocity profiles for various values of β.

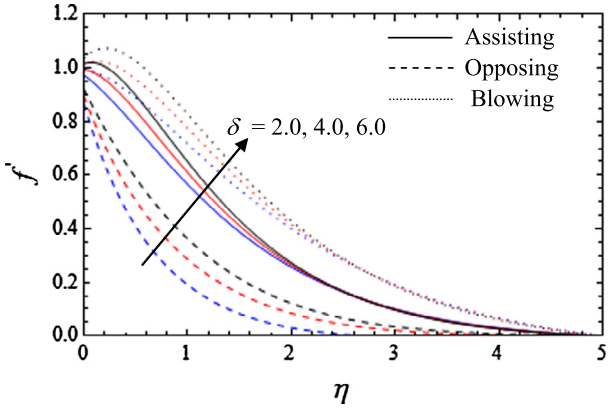

Figure 6 Velocity profiles for various values of δ.

graphically in Fig. 9 for different values of permeability parameter. It is found that an increase in the permeability enhances the temperature of the fluid. The influence of the radiation parameter on the temperature profiles for the cases of assisting, opposing and blowing are shown in Fig. 10, displaying the temperature enhancement with increase in radiation parameter. The variations in the temperature profiles for various Prandtl numbers are presented in Fig. 11. It is noticed that the temperature of the boundary layer diminishes with an increase in the Prandtl number. Fig. 12 gives some characteristic temperature profiles for different values of thermal slip parameter. It is seen that the temperature of the boundary layer reduces with an increase in the thermal slip parameter. Effects of inclination parameter on the temperature profiles are shown in Fig. 13. It is noticed that the thermal boundary layer thickness increases by increasing the angle of inclination [32].

The influences of Schmidt number on the concentration profiles is illustrated in Fig. 14. It is observed that the velocity

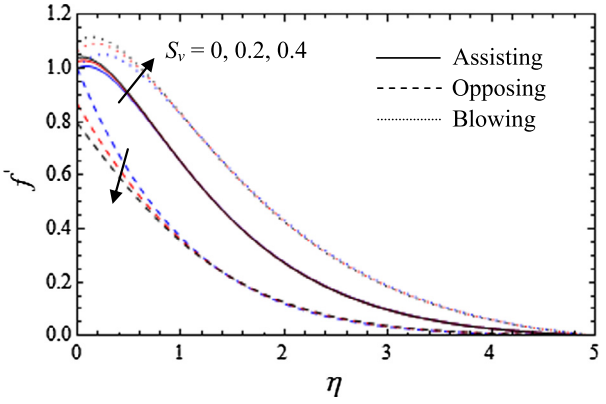

Figure 7 Velocity profiles for various values of S_v.

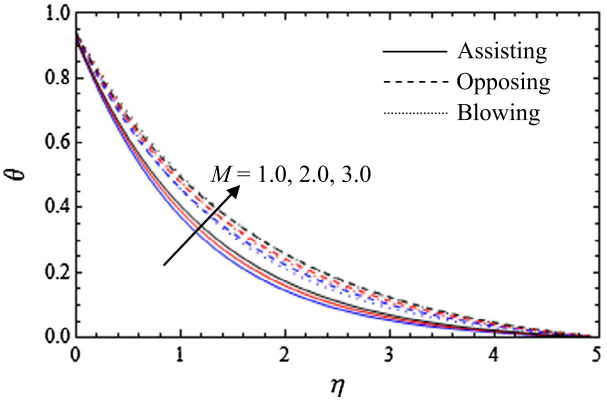

Figure 8 Temperature profiles for various values of M.

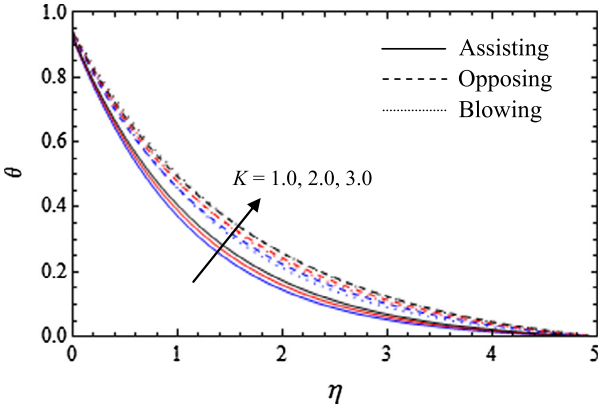

Figure 9 Temperature profiles for various values of k.

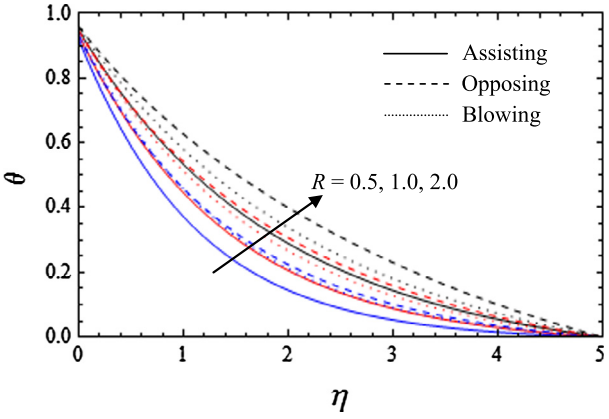

Figure 10 Temperature profiles for various values of R.

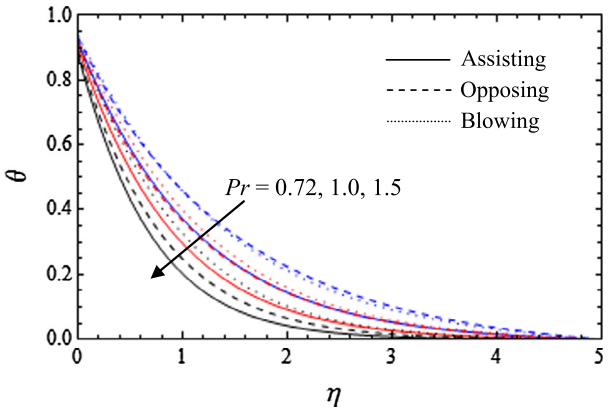

Figure 11 Temperature profiles for various values of Pr.

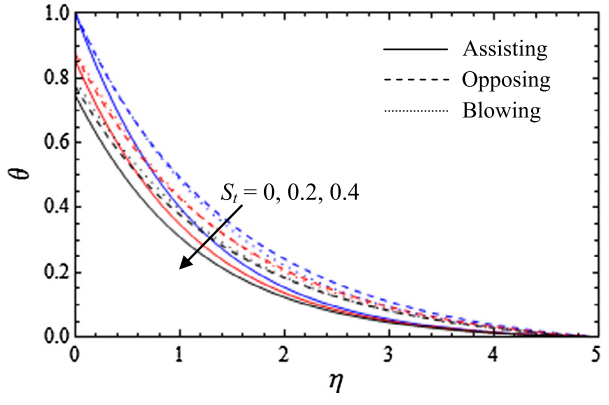

Figure 12 Temperature profiles for various values of S_t.

decreases as Schmidt number increases for the cases of assisting, opposing and blowing. The variation in the dimensionless concentration distribution for different values of inclination parameter is shown in Fig. 15 for the cases of assisting, opposing and blowing. It is observed that the concentration increases with the increase in the value of inclination parameter. Fig. 16 displays the effect of solutal slip on the concentration profiles. It reveals that the concentration profiles decrease with an increase in the solutal slip parameter. The effects of the chemical reaction parameter on the concentration for the cases of assisting, opposing and blowing are presented in Fig. 17. It is observed that the concentration decreases with increase in the value of chemical reaction parameter. Fig. 18 depicts some characteristic concentration profiles for different values of solutal buoyancy parameter. It is observed that concentration decreases with the increase in solutal buoyancy parameter.

The values of skin friction coefficient, Nusselt number and the Sherwood number for various values of the involved

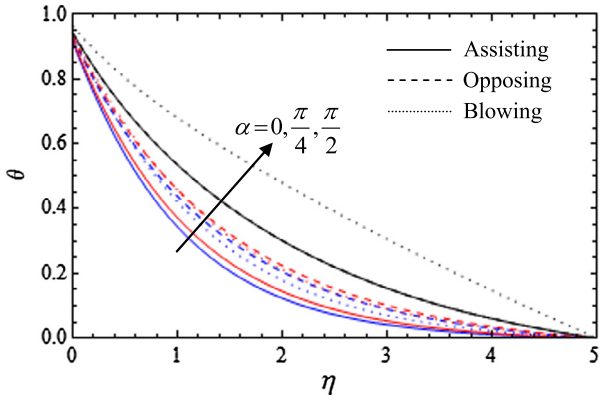

Figure 13 Temperature profiles for various values of α.

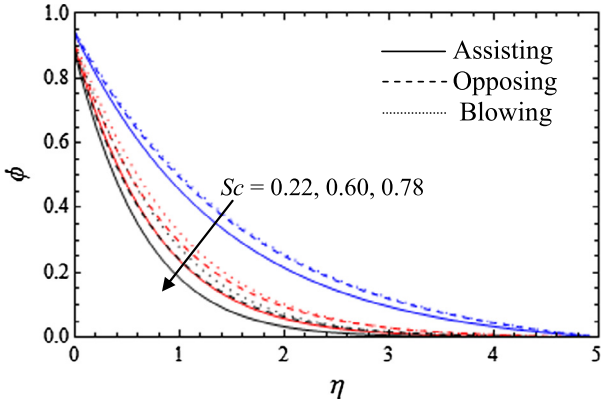

Figure 14 Concentration profiles for various values of Sc.

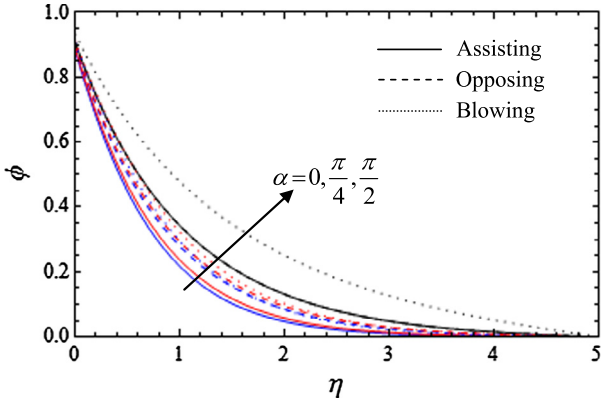

Figure 15 Concentration profiles for various values of α.

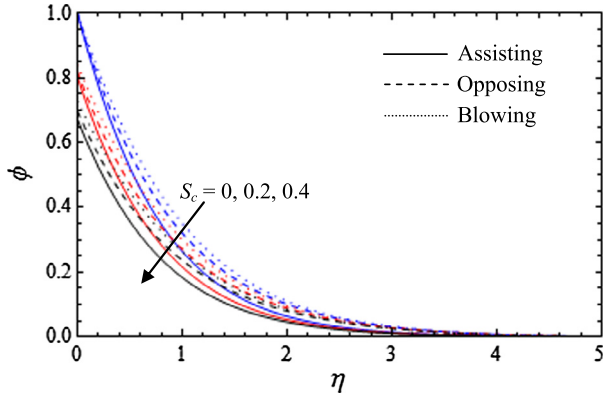

Figure 16 Concentration profiles for various values of S_c.

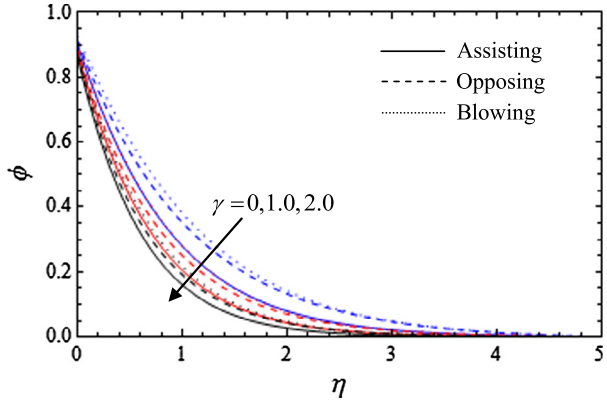

Figure 17 Concentration profiles for various values of γ.

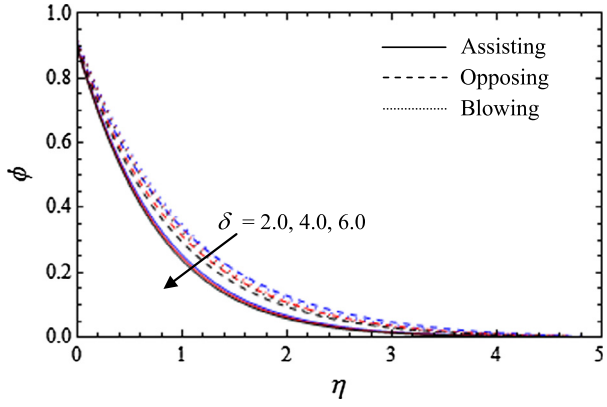

Figure 18 Concentration profiles for various values of δ.

pertinent parameters are presented in Tables 2 and 3. It can be noted that the skin friction coefficient decreases with the increase in values of Casson fluid parameter, magnetic parameter, permeability parameter, inclination parameter, suction parameter, slip velocity, Prandtl number, thermal slip, Schmidt number, chemical reaction parameter and solutal slip, whereas the reverse trend is observed in the case of buoyancy parameter, solutal buoyancy parameter and thermal radiation parameter. It is found that the Nusselt number decreases with an increase in the magnetic parameter, permeability parameter, inclination parameter, radiation parameter, thermal slip, Schmidt number, chemical reaction parameter and solutal slip, whereas it increases with an increase in the Casson fluid parameter, buoyancy parameter, solutal buoyancy parameter, suction parameter, slip velocity and Prandtl number. It is viewed that the Sherwood number decreases as the magnetic parameter, permeability parameter, inclination parameter, Prandtl number, thermal slip and solutal slip are increased. It can be seen that the Sherwood number increases with the increase in Casson fluid parameter, buoyancy parameter, solutal buoyancy parameter, suction parameter, velocity slip, radiation parameter, Schmidt number and chemical reaction parameter are raised.

5. Conclusions

The present investigation is a worthy attempt to study the magnetohydrodynamic convective boundary layer flow of a Casson fluid over an exponentially inclined permeable stretching surface in the presence of thermal radiation and chemical reaction. Numerical method is used to solve the resulting system of coupled nonlinear ordinary differential equations with boundary conditions. In light of the investigation, it is found that the momentum boundary layer thickness decreases with an increasing the Casson fluid parameter. It is observed that the opposite behavior of the temperature profile is observed for both thermal radiation parameter and the Prandtl number. It is seen that the same behavior of the concentration is found for the Schmidt number and chemical reaction parameter.

Acknowledgment

The author is grateful to the editor and reviewers for valuable suggestions and comments, which helped a lot to improve the quality of the paper.

References

[1] Prasad KV, Pal D, Datti PS. MHD power-law fluid and heat transfer over a non-isothermal stretching sheet. Commun Nonlinear Numer Simulat 2009;14:2178–89.
[2] Mahantesh MN, Subhas Abel M, Jagadish T. Heat transfer in a Walter's liquid B fluid over an impermeable stretching sheet with non-uniform heat source/sink and elastic deformation. Commun Nonlinear Numer Simulat 2010;15:1791–802.
[3] Hayat T, Awais M, Sajid M. Mass transfer effects on the unsteady flow of UCM fluid over a stretching sheet. Int J Mod Phys B 2011;25:2863–78.
[4] Nadeem S, Zaheer S, Fang T. Effects of thermal radiation on the boundary layer flow of a Jeffery fluid over an exponentially stretching surface. Numer Algor 2011;57:187–205.
[5] Sanjayanand E, Khan SK. On heat and mass transfer in a viscoelastic boundary layer flow over an exponentially stretching sheet. Int J Thermal Sci 2006;45:819–28.
[6] Mohamed Abd El-Aziz. Viscous dissipation effect on mixed convection flow of a micropolar fluid over an exponentially stretching sheet. Can J Phys 2009;87:359–68.
[7] Nadeem S, Mehamood R, Akbar NS. Non-orthogonal stagnation point flow of a nano non-Newtonian fluid towards a stretching surface with heat transfer. Int J Heat Mass Transf 2013;57:679–89.
[8] Akbar NS, Nadeem S, Rizwan Ul Haq, Shiwei Ye. MHD stagnation point flow of Carreau fluid toward a permeable shrinking sheet: dual solutions. Ain Shams Eng J 2014;5:1233–9.
[9] Nadeem S, Bushra Tahir, Fotni Labropulu, Akbar NS. Unsteady oscillatory stagnation point flow of a Jeffery fluid. J Aerosp Eng 2014;27:636–43.
[10] Fung YC. Biodynamics circulation. New York: Springer-Verlag Inc.; 1984.
[11] Dash RK, Mehta KN, Jayaraman G. Casson fluid flow in a pipe filled with a homogeneous porous medium. Int J Eng Sci 1996;34:1145–56.
[12] Nadeem S, Haq Rizwana UI, Lee C. MHD flow of a Casson fluid over an exponentially shrinking sheet. Sci Iran B 2012;19:1550–3.
[13] Hayat T, Shehzad SH, Alsaed A. Soret and Dufour effects on magnetohydrodynamic flow of Casson fluid. Appl Math Mech-Engl Ed 2012;33:1301–12.
[14] Hayat T, Shehzad SA, Alsaediz A, Alhothuali MS. Mixed convection stagnation point flow of Casson fluid with convective boundary conditions. Chin. Phys. Lett. 2012;29:114704-1–4.
[15] Mukhopadhyay S, Prativa Ranjan De, Bhattacharya K, Layek GC. Casson fluid flow over an unsteady stretching surface. Ain Shams Eng J 2013;4:933–8.
[16] Mustafa M, Hayat T, Pop I, Hendi A. Stagnation point flow and heat transfer of a Casson fluid towards a stretching sheet. Z Naturforsch 2012;67a:70–6.
[17] Mukhopadhyay S. Casson fluid flow and heat transfer over a nonlinearly stretching surface. Chin Phys B 2013;22:074701-1–5.
[18] Pramanik S. Casson fluid flow and heat transfer past an exponentially porous stretching surface in presence of thermal radiation. Ain Shams Eng J 2014;5:205–12.
[19] Bhattacharya K, Hayat T, Alsaedi A. Exact solution for boundary layer flow of Casson fluid over a permeable stretching/shrinking sheet. Z Angew Math Mech 2014;94:522–8.
[20] Hussanan A, Salleh MZ, Tahar RM, Khan I. Unsteady boundary layer flow and heat transfer of a Casson fluid past an oscillating vertical plate with Newtonian heating. PLoS One 2014;9:e108763.
[21] Nadeem S, Rashid Mehmood, Akbar NS. Optimized analytic solution for oblique flow of Casson-nano fluid with convective boundary condition. Int J Therm Sci 2014;78:90–100.
[22] Bidin B, Nazar R. Numerical solution of the boundary layer flow over an exponentially stretching sheet with thermal radiation. Eur J Sci Res 2009;33:710–7.
[23] Magyari E, Keller B. Heat and mass transfer in the boundary layers on an exponentially stretching continuous surface. J Phys D Appl Phys 1999;32:577–85.
[24] Mukhopadhyay S, Reddy GRS. Effects of partial slip on boundary layer flow past a permeable exponential stretching sheet in presence of thermal radiation. Heat Mass Transf 2012;48:1773–81.
[25] Ishak A. MHD boundary layer flow due to an exponentially stretching sheet with radiation effect. Sains Malaysiana 2011;40:391–5.
[26] Misra JC, Sinha A. Effect of thermal radiation on MHD flow of blood and heat transfer in a permeable capillary in stretching motion. Heat Mass Transf. 2013;49:617–28.
[27] Aboeldahab EM, Azzam GE-DA. Unsteady three-dimensional combined heat and mass free convective flow over a stretching surface with time dependent chemical reaction. Acta Mech 2006;184:121–36.

[28] Chamka AJ, Aly AM, Mansour MA. Similarity solution for unsteady Heat and Mass transfer from a stretching surface embedded in a porous medium with suction/injection and chemical reaction effects. Chem Eng Commum 2010;197:846–58.
[29] Pal D, Mondal H. MHD non-Darcy mixed convection heat and mass transfer over a non-linear stretching sheet with Soret–Dufour effects and chemical reaction. Int Commun Heat Mass Transfer 2011;38:463–7.
[30] Hernandez VR, Zueco J. Network numerical analysis of radiation absorption and chemical effects on unsteady MHD free convection through a porous medium. Int J Heat Mass Transfer 2013;64:375–83.
[31] Srinivas S, Reddy PBA, Prasad BSRV. Effects of chemical reaction and thermal radiation on MHD flow over an inclined permeable stretching surface with non-uniform heat source/sink: an application to the dynamics of blood flow. J Mech Med Biol 2014;14(1450067):1–24.
[32] Srinivas S, Reddy PBA, Prasad BSRV. Non-Darcian unsteady flow of a micropolar fluid over a porous stretching sheet with thermal radiation and chemical reaction. Heat Transfer-Asian Res; 2016. doi: http://dx.doi.org/10.1002/htj.21090 [in press].
[33] Kirubhashankar CK, Ganesh S. Unsteady MHD flow of Casson fluid in a parallel plate channel with heat and mass transfer of chemical reaction. Indian J Res 2014;3:101–5.
[34] Hussanan A, Ismail Z, Khan I, Hussein AG, Shafie S. Unsteady boundary layer MHD free convection flow in a porous medium with constant mass diffusion and Newtonian heating. Eur Phys J Plus 2014;129:1–16.
[35] Pramanik S. Casson fluid flow and heat transfer past an exponentially porous stretching surface in presence of thermal radiation. Ain Shams Eng J 2014;5:205–12.

P. Bala Anki Reddy was born and brought up in Andhra Pradesh, India. He obtained the M. Sc. and Ph.D. degrees in Mathematics from the Sri Venkateswara University, Tirupati, Andhra Pradesh. Presently, he is working as Assistant Professor, department of Mathematics, VIT University, Vellore, Tamilnadu. His research interest covers the areas of the application of flow separation, particularly, in bio-fluid dynamics and analysis of boundary layer flows of Newtonian/non-Newtonian fluids including the heat and mass transfer in porous/non-porous media. His research interest also covers the Nano fluid flow problems. He published several papers in national and international journals. He attended several workshops/seminars/faculty development programs.